Int. J. Heat Mass Transfer. Vol. 30, No. 3, pp. 469–478, 1987
Printed in Great Britain

0017 9310/87 $3.00 + 0.00
Pergamon Journals Ltd.

Thermal instability of evaporating drops on a flat plate and its effects on evaporation rate

NENGLI ZHANG,* B. X. WANG* and YOUREN XU†

* Thermal Engineering Department, Tsinghua University, Beijing 100084, China
† Physics Research Group, East China Technical University of Water Resources, Nanjing, China

(*Received* 7 *May* 1986)

Abstract—A number of pure and binary liquid drops evaporating on a flat plate were tested by optical methods. The difference of basic evaporation characteristics between the pure and binary liquid drops is revealed. The analysis of the instability of the interfacial flow for binary liquid drops is made and the surface phase mechanism of the formation of flow patterns is presented.

1. INTRODUCTION

THE EVAPORATION of liquid droplets on a flat plate is one of the universal phenomena in nature and in industrial processes. A comprehensive survey of the literature about this problem is available in refs. [1–3]. Usually, the vaporization of drops on a flat plate at higher temperatures attracted attention. However, the evaporation of drops on a solid surface at ambient temperature has recently been paid more attention [4–7] along with the development of chemical defence techniques related to the evaporative drying of chemical sprays from military equipment and with the growth of biological technology.

The present study is a continuation of a previous work [8], using a newly designed optical system [9] to investigate the interfacial flow patterns and to determine the evaporation rate of evaporating drops on a flat plate. The results of this study lead to the finding of the difference of basic characteristics between the pure and binary drops. A hypothesis of the so-called 'surface phase mechanism' is presented to explain the results of the experiments.

2. EXPERIMENTAL APPARATUS AND PROCEDURE

The new real-time holographic interferometry apparatus used is shown in Fig. 1 [9]. The laser beam was filtered, collimated, and then reflected onto the double holographic grating which was made from two holographic gratings arranged parallel, in tandem with a small intersectional angle 2δ between their grating lines. The beam passed through the double holographic grating and was diffracted into two sets of diffraction modes. The two first-order diffraction modes, diffracted respectively by two gratings, would have an intersectional angle 2θ and were chosen as the working beams, as illustrated in Fig. 2. These two beams were adjusted by turning mirror I or the double holographic grating to shine symmetrically on the emulsion plane of the holographic plate. Exposure of the holographic plate was carefully controlled by the electric shutter, the plate was then developed and replaced accurately using the replacement device. The liquid drop was placed on the glass plate which had been laid on the replaced holographic plate and exposed to the beams, a set of moire fringes was formed on the emulsion plane by two sets of gratings, obtained respectively from the interferences between the two beams before and after the liquid drop was positioned. Mirror II and two lenses were used to obtain a horizontally enlarged view of the fringe images. A video cassette recorder or movie camera can record the change in the set of moire fringes. A special procedure was developed to calculate the volume–time history from the moire fringe movies [8]. It is better to change the angle 2δ for different liquid drops so as to obtain proper moire fringes. The relation between the angles 2δ and 2θ had been derived as [9]

$$2\theta = \delta\lambda f \tag{1}$$

where λ is the wavelength of the laser beam and f the spatial frequency of the gratings.

3. INSTABILITY OF INTERFACIAL FLOW

Eleven volatile, analytically pure organic liquids and their 41 binary systems were tested. Just as was pointed out in ref. [4], the pure liquid drops exhibited so-called stable- or substable-interface type evaporation except ethanol, methanol and acetone which absorb water vapor in the ambient to form binary mixtures during their evaporation processes. The recorded moire fringe movies, such as shown in Fig. 3, indicate that different binary drops may have different modes of evaporation. The evaporating drop will be stable in interfacial evaporation if the moire

NOMENCLATURE

A	partial mole surface area [$cm^2\,gmol^{-1}$]
d_e	equivalent diameter of liquid drop [cm]
f	spatial frequency of grating [μm^{-1}]
N_{cr}	dimensionless crispation number
N_e	dimensionless excessive free-energy of surface, defined in equation (2)
N_0	Avogadro number (6.023×10^{23}) [$gmol^{-1}$]
R	universal gas constant (8.314×10^4) [$ergs\,gmol^{-1}\,K^{-1}$]
T	temperature of liquid drop [K]
V	mole volume of liquid drop [$cm^3\,gmol^{-1}$]
X	mole fraction of component in binary drop.

Greek symbols

α	thermal diffusivity [$cm\,s^{-1}$]
δ, θ	angles defined in Fig. 2 [rad]
λ	wavelength of laser beam (0.6328) [μm]
σ	surface tension of liquid, [$dyn\,cm^{-1}$]
μ	dynamic viscosity of liquid [$g\,s^{-1}\,cm^{-1}$].

Subscripts

a, b	components a and b, respectively
m	binary liquid.

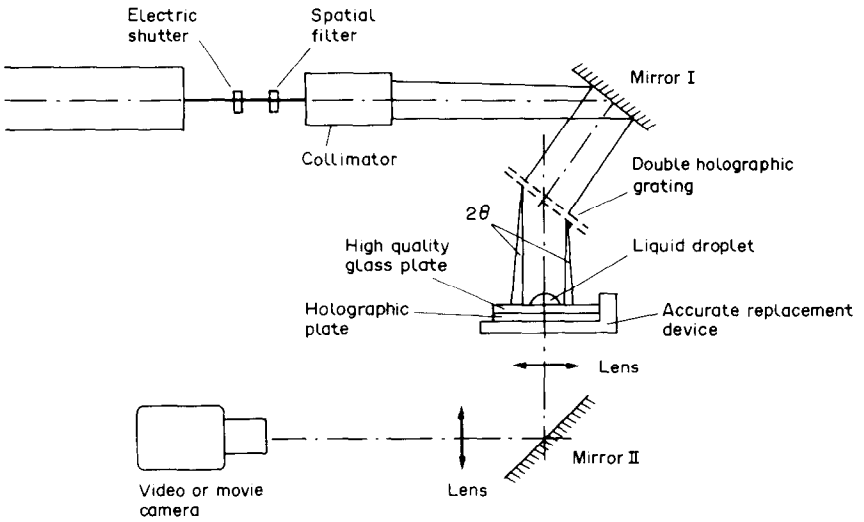

FIG. 1. Scheme of experimental apparatus.

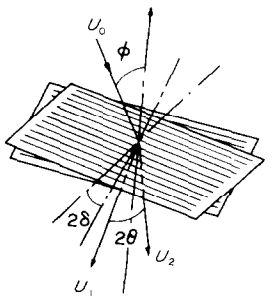

FIG. 2. Double holographic gratings as a beam splitter.

fringes remain a perfect symmetrical pattern. Otherwise, it will be unstable in interfacial evaporation. The 'perfect symmetrical pattern' of the moire fringes stands for a perfect spherical segment with a very smooth surface. A typical example of such kind of binary drops is illustrated in Fig. 3(a). Figures 3(b) and (c) are pictures of the moire fringes at different moments for unstable evaporation processes. It appears that the droplet surfaces are varying from smooth to rippled and the figures of the droplet become continuously irregular. The drop profiles at any given instant can be calculated according to the method reported in refs. [8, 10], and the results thus calculated are plotted in Fig. 4.

Two dimensionless parameters were found to play the major roles in driving interfacial instability [8]. One is the so-called 'dimensionless excessive free-energy of the surface'

$$N_e = (\Delta\sigma)^2 X_a X_b A/(2RT\sigma_m) \tag{2}$$

where $\Delta\sigma$ is the difference in the surface tensions of the pure liquid components in the binary liquids; X_a and X_b, the mole fractions of components a and b, respectively; A, the partial mole surface area which

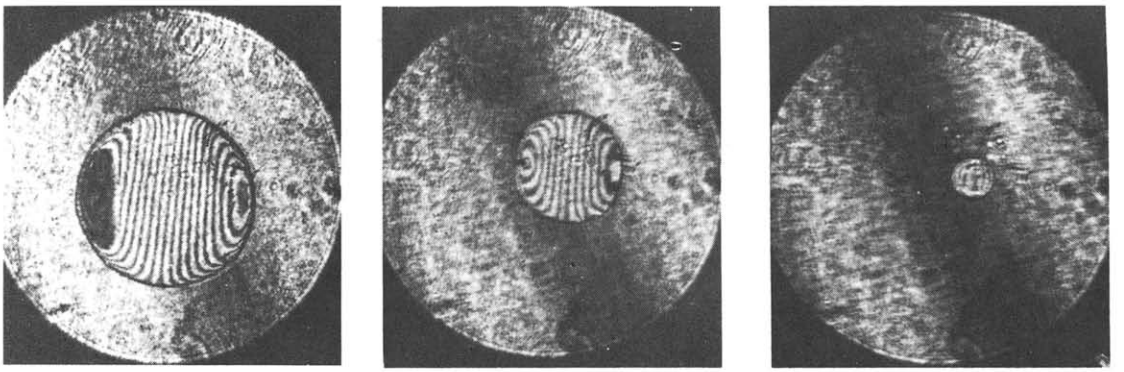

(a) 50% volume $CHCl_3$–50% volume CCl_4

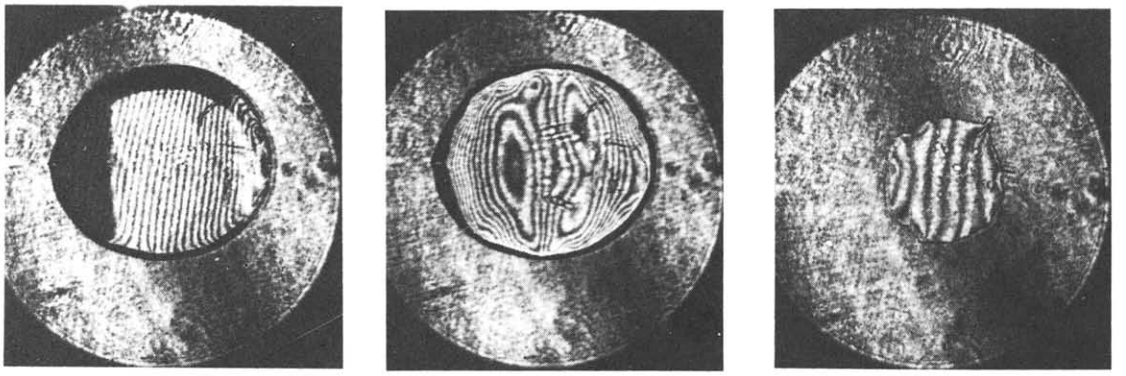

(b) 50% volume $CHCl_3$–50% volume C_2H_6O

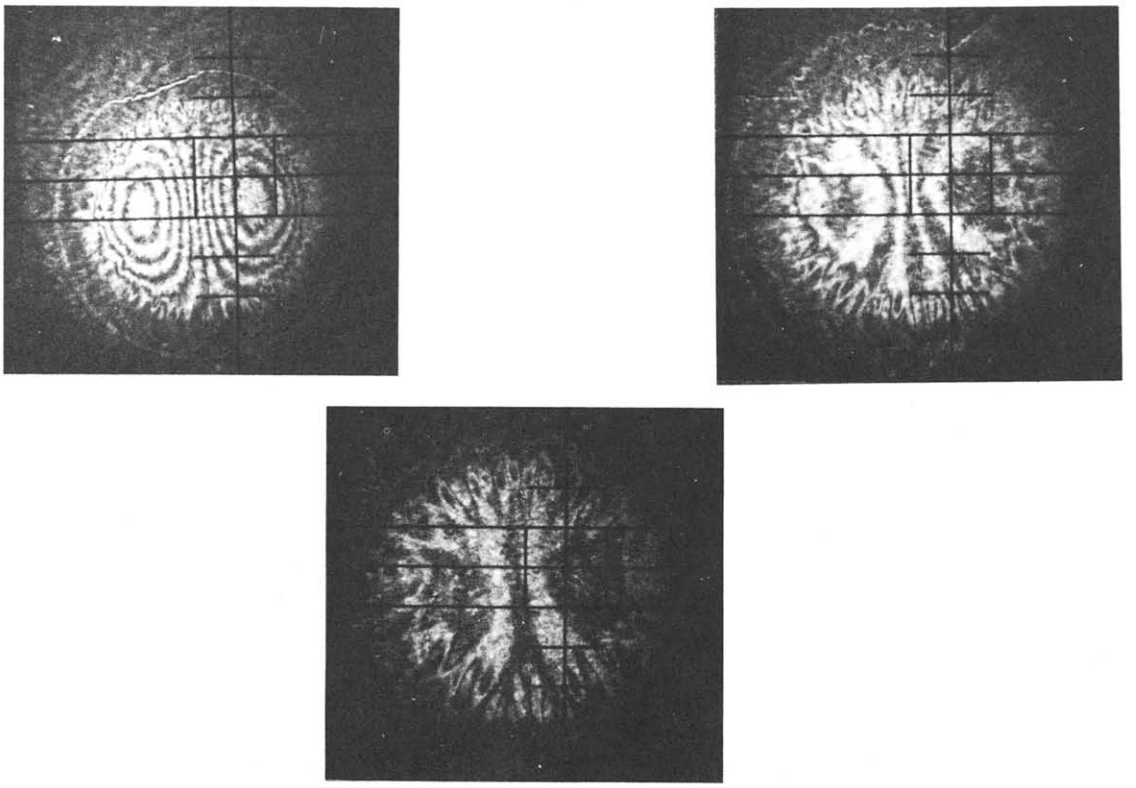

(c) 90% volume $(CH_3CH_2)_2O$–10% volume $CHCl_3$

FIG. 3. Moire fringes at different moments during evaporation processes.

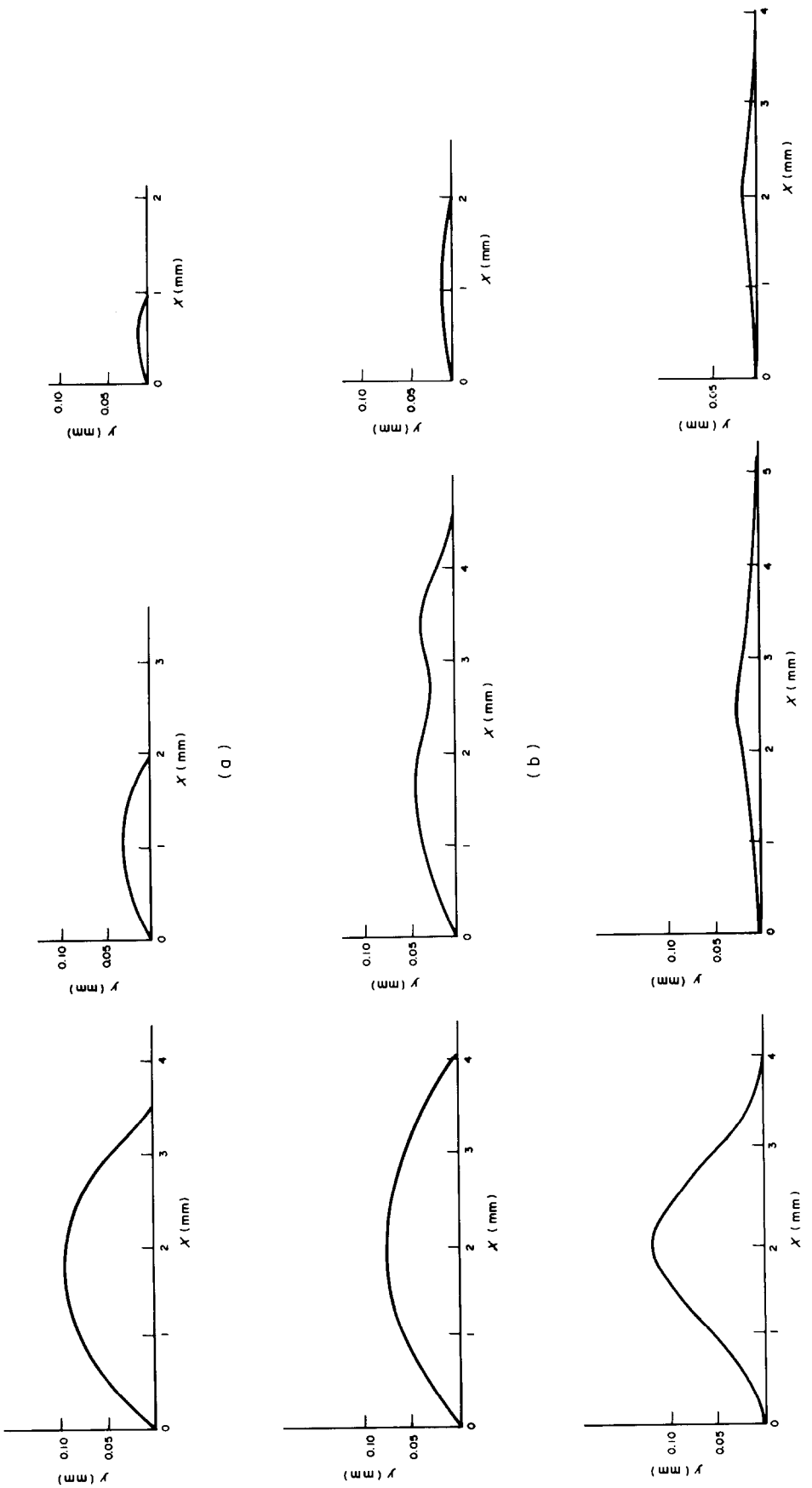

FIG. 4. Drop profile corresponding to moire fringes in Fig. 3.

Table 1.

Binary liquid	$N_e \times 10^3$	$N_{cr} \times 10^5$
1. Ethyl acetate–benzene	8.251	9.550
2. Benzene–cyclohexane	3.768	11.416
3. Ethyl acetate–chloroform	3.498	8.142
4. Ethyl acetate–carbon tetrachloride	3.303	10.088
5. Ethyl acetate–methylene chloride	2.047	6.971
6. Benzene–methylene chloride	1.511	8.604
7. Benzene–carbon tetrachloride	1.612	11.818
8. Ethyl acetate–cyclohexane	0.970	9.746
9. Chloroform–cyclohexane	0.890	9.233
10. Benzene–chloroform	0.898	9.150
11. Carbon tetrachloride–cyclohexane	0.729	12.055
12. Cyclohexane–methylene chloride	0.307	7.937
13. 10% methylene chloride–90% chloroform	0.050	7.724
14. 30% methylene chloride–70% chloroform	0.101	7.365
15. Methylene chloride–chloroform	0.105	6.965
16. 70% methylene chloride–30% chloroform	0.077	6.706
17. 90% methylene chloride–10% chloroform	0.029	6.406
18. Methylene chloride–chloroform	0.052	8.894
19. Chloroform–carbon tetrachloride	0.011	10.287
20. 10% ethyl ether–90% ethyl acetate	6.421	7.895
21. 10% cyclohexane–90% ethyl acetate	0.321	8.470
22. 5% ethyl acetate–95% cyclohexane	0.201	11.230
23. 10% ethyl ether–90% methylene chloride	5.954	5.605
24. 10% ethyl ether–90% chloroform	9.723	7.505
25. 20% ethyl ether–80% chloroform	19.137	7.153
26. 25% ethyl ether–75% chloroform	23.539	6.933
27. Ethyl ether–chloroform	40.796	6.345
28. 70% ethyl ether–30% chloroform	42.680	6.588
29. 90% ethyl ether–10% chloroform	22.870	6.036
30. Ethyl ether–benzene	56.565	7.944
31. Ethyl ether–carbon tetrachloride	45.490	8.283
32. Ethyl ether–cyclohexane	33.356	8.148
33. Ethyl ether–methylene chloride	31.166	5.269
34. Ethyl ether–ethyl acetate	21.760	6.864
35. 10% ethyl ether–90% benzene	13.987	10.486
36. 10% ethyl ether–90% carbon tetrachloride	11.769	12.230
37. 10% ethyl ether–90% cyclohexane	10.633	10.665
38. Alcohol–acetone	0.268	13.211
39. Methane–alcohol	0.0048	17.446
40. Alcohol–chloroform	5.557	12.899
41. 95% alcohol–5% water	347.10	25.376

All of the mixture ratios in the table are determined as the percentage by volume.

The mixture ratio not indicated in the table indicates a 50% volume–50% volume mixture.

is the average of those values for the pure components in the mixture and equal to $(V_a^{2/3} + V_b^{2/3})/(2N_0^{1/3})$, with V_a and V_b standing for the mole volumes of pure liquid components a and b, respectively; N_0, the Avogadro number; R, the universal gas constant; T, the temperature of droplet; and σ_m, the surface tension of the binary liquid.

Another parameter is the 'dimensionless crispation number'

$$N_{cr} = \mu_m \alpha_m / \sigma_m d_e \qquad (3)$$

where μ_m and α_m are the dynamic viscosity and the thermal diffusivity of the binary liquid; and d_e, the equivalent diameter of a drop on the test plate at zero time. The calculated values of N_e and N_{cr} for the 41 tested binary drops are listed in Table 1. The first 24 liquids in the table exhibited stable evaporation and the others exhibited unstable evaporation. An interfacial flow map has been constructed in Fig. 5 so as to divide the domains of the two basic interfacial flow patterns.

It is also found from calculations that the unstable evaporating drops possess higher dimensionless evaporation rates than the stable ones. As shown in Table 1 and Fig. 5, the binary mixture of ethyl ether–chloroform spanned both domains depending on the mixture ratio. Figures 6(a) and (b) are the moire fringes taken at sequential moments for binary drops of 10% volume ethyl ether–90% volume chloroform and for 20% volume ethyl ether–80% volume chloroform (serial Nos. 24 and 25 in Table 1 and Fig. 5), respectively. The transformation of evaporation patterns occurs just between these two binary drops with different mixture ratios.

4. LIFETIMES OF BINARY DROPS

When two pure liquids are blended to form a binary liquid, the behaviour of the molecules in the surface phase of the binary liquid depend strongly on the molecular structures. It is well known that the molecules of organic liquids possess more or less polarity according to the space arrangements between their atoms. For example, the molecule of carbon tetrachloride is nonpolarized because of its symmetrical structure and its dipole moment is equal to zero. However, the molecules of chloroform, methylene chloride and ethyl ether are polarized and have dipole moments of 1.01, 1.60 and 1.15 D, respectively, where

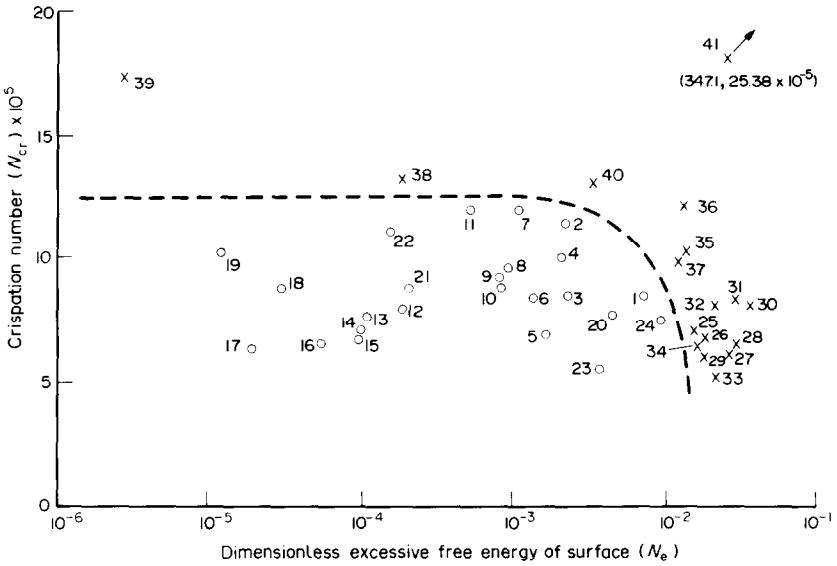

FIG. 5. Interfacial flow map for binary drops.

$D = 10^{-18}$ e.s.u. × cm [11]. Hence, an interesting fact is discovered that the lifetimes of binary drops will be not always linearly related to their mixture ratios, and three typical curves for the relations between the normalized lifetime and the mixture ratio are plotted in Fig. 7, where τ is the lifetime of the tested drop and τ_0 is the lifetime of the drop of less volatile pure liquid in the mixture.

If the liquid with polarized molecules is mixed with the liquid with nonpolarized ones, no ordered arrangement appeared at the surface phase, and therefore, its characteristics would be the same as the surface phase of pure liquids. This is the case for binary drops of chloroform–carbon tetrachloride whose lifetime is expected to be a linear function of the mixture ratio, as shown in Fig. 7(c).

If two liquids with polarized molecules are mixed together, the surface phase will be different from the bulk phase in properties. Two possible cases may exist, shown in Figs. 7(a) and (b), and can be analysed by the 'surface phase mechanism'.

5. SURFACE PHASE MECHANISM

The molecules of binary drops, with nearly similar physical properties and with not much difference in evaporation rates, would have almost equal abilities to occupy a position in the surface phase and would thus take on an alternating arrangement to form a monomolecular layer (or simply 'monolayer'), as shown in Fig. 8(a). Such a monolayer would have higher tightness than the surface layer of pure liquid. The increased Van der Walls' force in surface phase lessens the evaporation rate; it may be the reason for the variation of the lifetime curve from linear relation to uprise as in Fig. 7(b).

On the other hand, if a component in binary liquids, for example ethyl ether in the binary liquid of ethyl ether–chloroform, is much more volatile than the other component, its molecules will easily occupy the surface phase. When the volume fraction of this component reaches some level, its molecules would accumulate at many local areas. These accumulated molecules would take a parallel arrangement in the surface phase to form the monolayer under the action of the molecules in bulk phase, and repulsive pressure will appear in the monolayer, as shown in Fig. 8(b), to act as a force against surface tension. If the repulsive pressure exceeds the surface tension, the net effect causes the surface to expand and leads to rippling of the surface [12]. The effect will doubtless propagate to the boundary of the drop, and tends to spread if it is large enough to overcome the coherence with the solid surface, as shown in Fig. 9(a). If it cannot overcome the coherence with the solid surface, the boundary of the drop will not migrate but the buckling of the surface will be augmented to form an irregular surface figure, as shown in Fig. 9(b). Both these two patterns of surface expansion are inevitably accompanied with a convection in the drop and greatly enhance the evaporation rate. That may be why the lifetime curve in Fig. 7(a) bends downwards.

A conspicuous feature of Fig. 7(a) is that the lifetime curve first bends up and then down. The reason may also be found from the surface phase mechanism mentioned above. When the volume fraction of ethyl ether in the binary liquid drop is less than 20%, the number of molecules of ethyl ether may not be large enough to form the local accumulation at the surface of the drop even though it may occupy the surface phase more easily. In such a case, the molecules of ethyl ether and of chloroform would form a monolayer [Fig. 8(a)] and tend to lessen the evaporation rate. On the contrary, when the volume fraction of ethyl

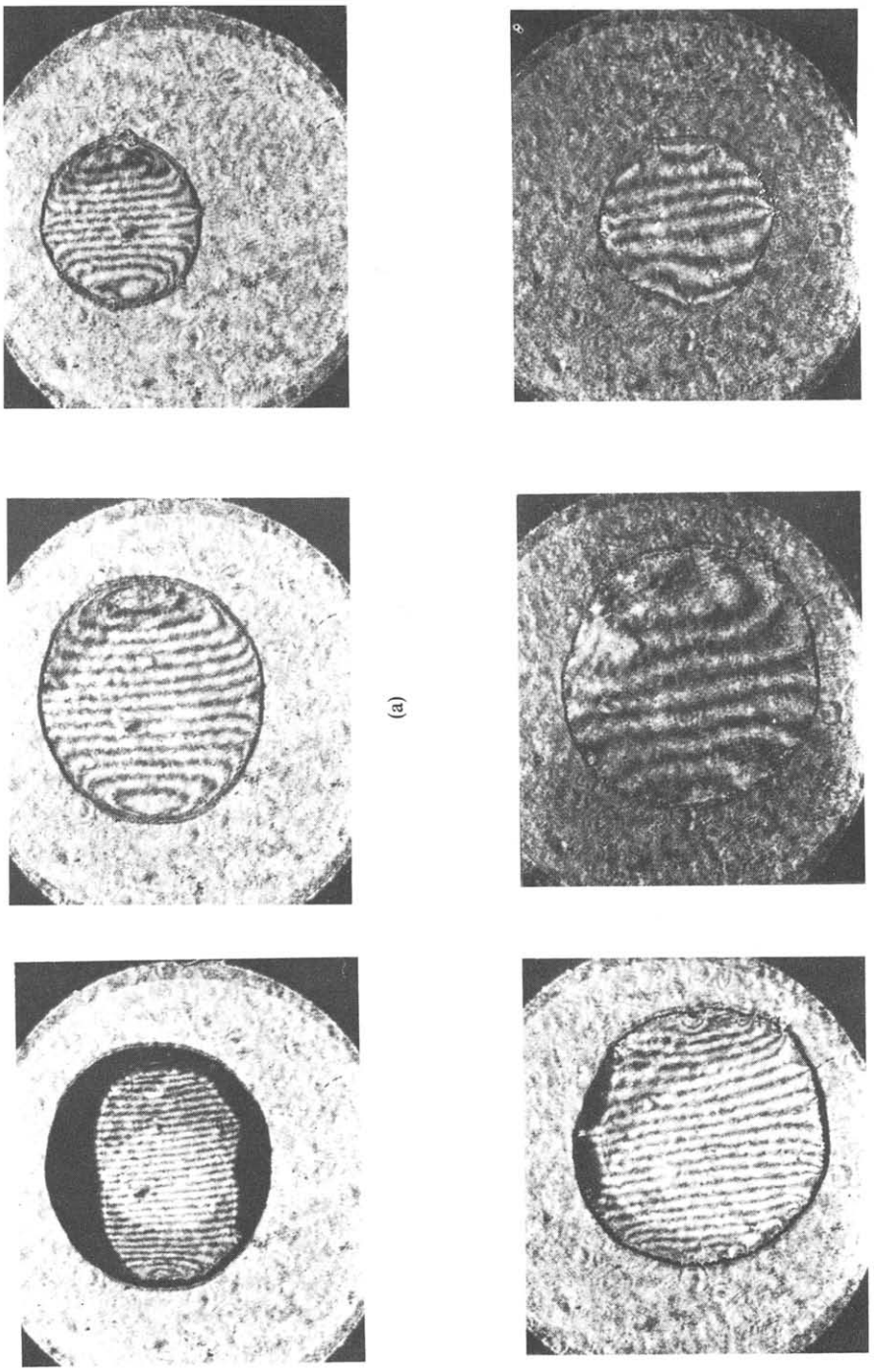

FIG. 6. Transformation of evaporation patterns.

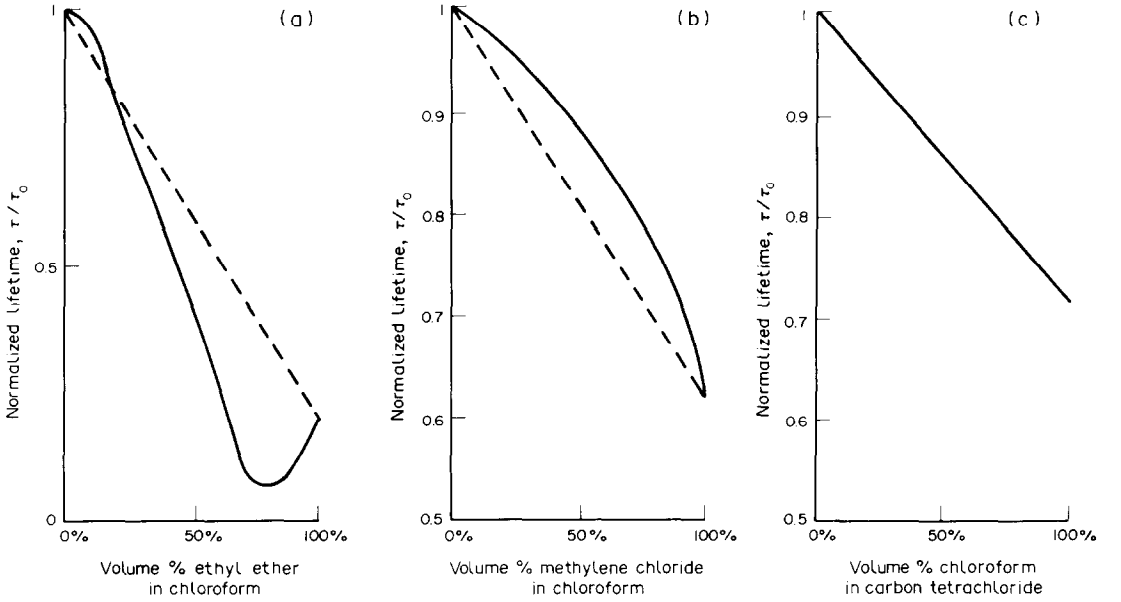

FIG. 7. Lifetime–mixture ratio curves for binary drops (10 μl).

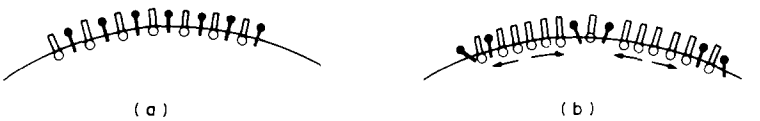

FIG. 8. Monomolecular layer.

ether reaches or exceeds 20%, the monolayer [Fig. 8(b)] would be created and the evaporation rate would be enhanced by the interface turbulence. This coincides with the concentration (mixture ratio) effect on stability mentioned above.

This mechanism not only explains the change of evaporation pattern with the mixture ratio for a binary drop, but also can be used to interpret why some liquids may have a higher evaporation rate in wet than in dry air.

6. CONCLUSIONS

A new real-time holographic interferometry set-up has been used to investigate the drop evaporation processes of 11 pure organic volatile liquids and their 41 binary systems. The moire fringe movies of the drops give comprehensive information about the processes, exposing the different characteristics of evaporation between the pure liquid drops and the binary drops and exploring two basic evaporation patterns for the binary drops on a flat plate.

Two dimensionless parameters, crispation number and dimensionless excessive free-energy of surface, are used to construct the interfacial flow map of evaporation for binary drops.

The surface phase mechanism is used successfully to explain the formation of two difference patterns of drop evaporation on a flat plate and to interpret three different kinds of lifetime–mixture ratio curves for the binary drops.

All of these are useful in understanding the evaporating nature and the characteristics of binary drops on a flat plate, which are related to several practical engineering problems, such as distillation, evaporation, combustion.

Acknowledgements—Project supported by the Science Fund of the Chinese Academy of Sciences, Beijing (Grant No. TS 840220) and by the Research Fund of the Ministry of Education, China (Grant No. 850154/080024).

REFERENCES

1. W. J. Yang, Theory on evaporation and combustion of liquid drops of pure substances and binary mixtures on heated surface, ISAS Report No. 535 (Vol. 40, No. 15), Institute of Space and Aeronautical Sciences, University of Tokyo, Japan (1975).
2. Nengli Zhang and W. J. Yang, Evaporation and explosion of liquid drops on a heated surface, *Exp. Fluids* **1**, 101–111 (1983).
3. R. F. Mann and W. W. Walker, The vaporization of small binary drops on a flat plate at maximum heat flux, *Can. J. chem. Engng* **53**, 487–493 (1975).

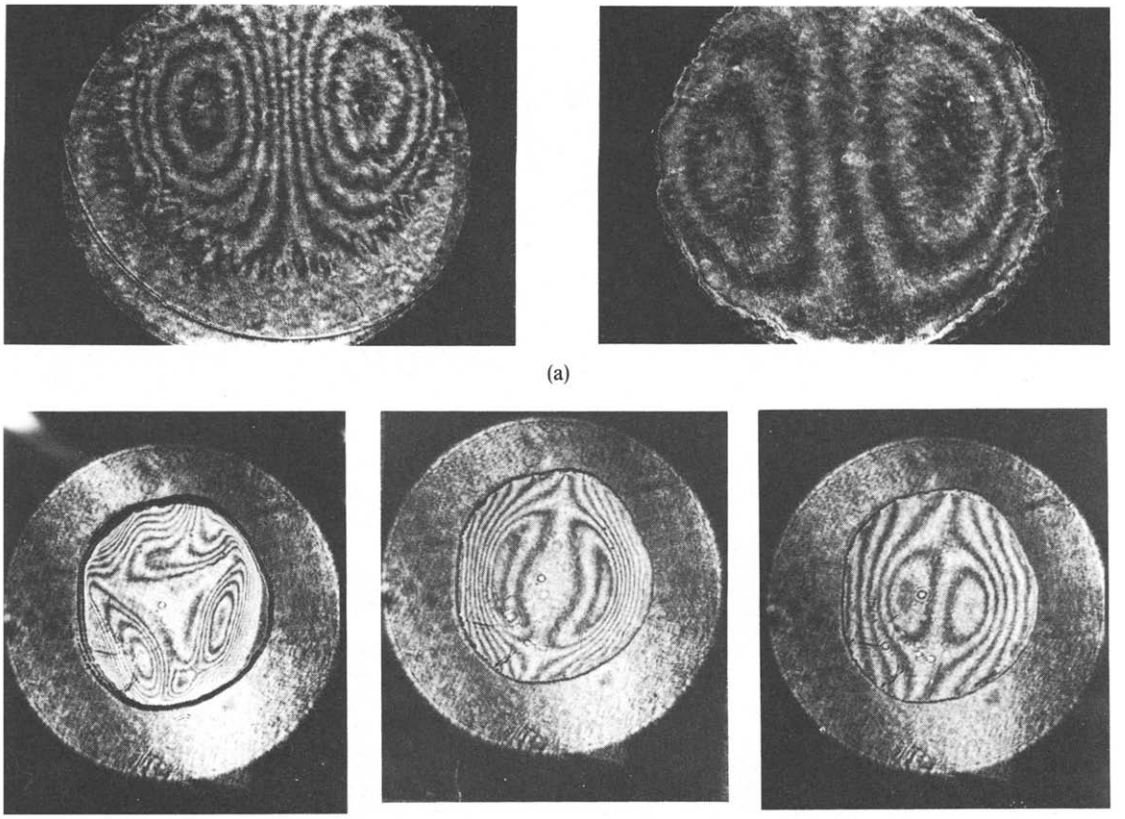

(a)

(b)

FIG. 9. Surface expansion of binary drops.

4. Nengli Zhang and W. J. Yang, Natural convection in evaporating minute drops, *J. Heat Transfer* **104**, 565–662 (1982).
5. Nengli Zhang and W. J. Yang, Micro-structure of flow inside minute drops evaporating on a surface, *J. Heat Transfer* **105**, 908–910 (1983).
6. Youren Xu, Nengli Zhang, W. J. Yang and C. M. Vest, Optical measurement of profile and contact angle of liquids on transparent substances, *Exp. Fluids* **2**, 142–144 (1984).
7. Nengli Zhang and W. J. Yang, Interfacial flow and evaporation of sessile drop on as vertical surface, *J. Heat Transfer* **106**, 652–656 (1984).
8. Nengli Zhang, Youren Xu and W. J. Yang, Thermal stability in binary droplet vaporation on a flat plate by real-time holographic interferometery, *Proceedings of the Eighth International Heat Transfer Conference*, San Francisco, Vol. 2, pp. 525–530 (1986).
9. Youren Xu, Nengli Zhang and B. X. Wang, Real-time grating shearing interferometry applied to investigating of evaporative convection in liquid drops, *Appl. Laser* **6**, 145–149 (1986), in Chinese.
10. Youren Xu and Nengli Zhang, Droplet profile measurement with holographic interferometry, *Int. Symposium on Fluid Control and Measurement*, Tokyo (1985).
11. J. A. Dean (Editor), *Lange's Handbook of Chemistry*, 12th edn. McGraw-Hill, New York (1979).
12. J. T. Davies and E. K. Rideal, *Interfacial Phenomena*, 2nd edn. Academic Press, New York (1963).

INSTABILITES THERMIQUE DE GOUTTES S'EVAPORANT SUR UNE PLAQUE PLANE ET SES EFFETS SUR LA VITESSE D'EVAPORATION

Résumé—Un certain nombre de gouttes liquides pures ou binaires, en évaporation sur une plaque plane, est étudié par des méthodes optiques. On observe la différence des caractéristiques d'évaporation entre les liquides pures et binaires. On présente l'analyse de l'instabilité de l'écoulement interfacial pour des gouttes liquides binaires et on décrit le mécanisme de formation des configurations d'écoulement.

THERMISCHE INSTABILITÄT BEI DER VERDAMPFUNG VON TROPFEN

Zusammenfassung—Die Verdampfung einer Anzahl reiner und binärer Flüssigkeitstropfen an einer ebenen Platte wurde mit optischen Verfahren beobachtet. Der Unterschied zwischen reinen und binären Stoffen im Hinblick auf das grundlegende Verdampfungs-Verhalten wird aufgezeigt. Für binäre Flüssigkeitstropfen wird die Instabilität der Grenzflächenströmung analysiert und der Mechanismus der Ausbildung der Strömungsformen dargestellt.

ТЕРМИЧЕСКАЯ НЕУСТОЙЧИВОСТЬ ИСПАРЯЮЩИХСЯ КАПЕЛЬ НА ПЛОСКОЙ ПЛАСТИНЕ И ЕЕ ВЛИЯНИЕ НА СКОРОСТЬ ИСПАРЕНИЯ

Аннотация—Оптическими методами исследовалось испарение на плоской пластине капель ряда чистых и бинарных жидкостей и установлено различие в основных характеристиках их испарения. Проведен анализ неустойчивости течения на межфазной границе для капель бинарных жидкостей и описан механизм формирования картин течения под влиянием поверхностных эффектов.